



Red Beet Peel-Loaded Liposome's Impact on Metabolic Syndrome Rats and Its Use as Fortifier in Yoghurt Powder

Moetazza M. Alshafei^{1*}, Dina Mostafa Mohammed¹, Emtenan M. Hanafi³, Seham S.

Kassem¹, Tamer M. El-Messery², Reda M. S. Korany⁴, Marwa M. El-Said².

^{1.} Department of Nutrition and Food Science, National Research Centre, Dokki, Giza, Egypt

^{2.} Department of Dairy, National Research Centre, Dokki, Giza, Egypt

^{3.} Department of Animal Reproduction, National Research Centre, Dokki, Giza, Egypt.

^{4.} Department of Pathology, Faculty of Veterinary Medicine, Cairo University, Giza, Egypt



CrossMark

Abstract

Metabolic syndrome (MetS) is associated with dyslipidemia, high blood pressure, type II diabetes and other complications. The red beet peels rich in antioxidant that may control metabolic syndrome. Microencapsulation increase pharmaceutical compound bioavailability. The study aimed to evaluate the effects of red beet peel loaded liposomes (RBPL) on MetS rats and the production of yoghurt powder fortified with RBPL as functional food. RBPL was produced, microcapsules characterization was studied. 30 sprague dawely female rats were divided into 3 groups (N=10), control(C) fed on basic diet, (MetS) fed on high fat high carbohydrates diet (HFD) and (RBPL) fed on HFD and RBPL for 60 days. Animals were euthanized, body and internal organs were weighed and the organs were collected for histopathology and Immunohistochemistry for iNOS and Caspas-3 markers. Plasma was collected for biochemical analysis of parameters related to MetS. Freeze-dried yoghurt powders containing RBPL was produced. Results showed high encapsulation efficiency of RBPL which were stable and evenly distributed. The RBPL fortified yoghurt powder showed characterization as control yoghurt. There were significant increase in glucose, lipids, liver and kidney profiles, leptin, irisin and malondialdehyde in MetS group, decrease in high density lipoprotein, albumin, catalase, total antioxidant, T3, TSH, insulin, IGF, phosphorus and zinc when compared to (C). Histopathologic sections showed derangement of tissues in organs with MetS and high expression of iNOS and caspase-3. RBPL took all the disrupted findings towards normal. This study showed RBPL's health benefits on MetS and were applied as fortifier in dried yoghurt powder.

Keywords: metabolic syndrome, red beet peel, liposomes, yoghurt powder, liver steatosis, polycystic ovary, immunohistochemistry.

1. Introduction

The metabolic syndrome (MetS) is a complex disorder characterized by central (abdominal) obesity, hyperlipidemia, high blood pressure, and type II diabetes. Combination of three of them confirms the diagnosis [1]. Prevalence of MetS is steadily rising, which predisposes to diabetes, cardiovascular disease, fertility problem and liver disorder, this has triggered public concern in many countries [2]. Oxidative stress is the main triggering factor that stands behind metabolic syndrome [1-3]. Cardiovascular events and ovarian dysfunction are complication of MetS. Diabetes and

obesity significantly triggers oxidative stress, which in turn leads to DNA damage which suppresses ovum maturation in ovaries [4-5]. Red beet peel (RBP) is rich in betalain which have high antioxidant effect that counteracts the inflammatory process associated with MetS [2-3,6-7]. The red beet peel (RBP) has 50 % phenolic compounds, whereas the RB core contains only 13 %. The European Union has approved red beet concentrate as a food ingredient and colorant in all food applications, and it is labeled as E162 [8]. However, the stability of the antioxidant compounds may be reduced during processing and storage. Liposome-based delivery systems with its unique lipid bilayer structure improve the cellular

*Corresponding author e-mail: moetazza1_alshafei@yahoo.com

Receive Date: 23 March 2022, Revise Date: 19 May 2022, Accept Date: 30 May 2022

DOI: 10.21608/EJCHEM.2022.129208.5714

©2023 National Information and Documentation Center (NIDOC)

transport and bioavailability of sensitive bioactive food components and protect them from environmental reactions[9-10]. Characterization of liposome is essential to verify the efficiency of microencapsulation[11]. Yoghurt can be fortified by antioxidant compounds and freeze dried to act as functional food for human consumption [12]. This study aimed to prepare red beet peel liposomes to improve the stability of phenolic compounds, to investigate its effect on metabolic syndrome risk factors in rat model. The preparation of dried yoghurt fortified by the RBP liposomes was another target.

2- Materials and Methods

The red beet (*Beta vulgaris* L) was bought from an Egyptian local market and was carefully selected for defects before being washed and peeled. Soy lecithin (69.3% phosphatidyl choline, 9.8% phosphatidylethanolamine, and 2.1% lysophosphatidyl choline) (Ludwigshafen, Germany). Merck provided all of the chemicals (Darmstadt, Germany).

Determination of total phenolic compounds

The extraction of phenolic compounds from red beet was carried out [13]. The total phenolic content was determined [14]. The results were expressed as mg of catechin equivalent per ml.

Determination of total antioxidant activity

The antioxidant activity was determined by the ability of antioxidants to scavenge DPPH (2,2-diphenyl-1-picrylhydrazyl) as a free radical [15].

Production of red beet peel extract loaded liposomes (RBPL)

Liposomes were formed. To achieve complete dissolution and homogeneity, 2% of soy lecithin powder was dissolved in 100 ml acetate buffer (250 mM, pH 3.5) and stirred overnight. RBP powder was added to the soy lecithin solutions in various concentrations (0.2, 0.4, 0.6, 0.8, and 1%). Ultrasonication (Sonics, Vibra, Cell, USA) was applied to homogenize RBP liposomes solutions for 15 minutes. After that, the liposomes were stored in amber bottles and kept at 4 °C in the refrigerator [11].

Characterizations of liposomes

A. Size distribution, ζ-Potential and polydispersity index

Using a Dynamic Light Scattering (DLS) device (Zetasizer Nano ZS, Malvern Instruments, UK) equipped with a He—Ne laser at a wavelength of 633 nm, liposomes were evaluated in terms of size distribution (by number), polydispersity index.

B. Encapsulation efficiency

Encapsulation efficiency (EE) was determined through the separation of the loaded particles from free phenolic compounds (FPC) extract. Encapsulation efficiency was calculated as equation [11].

$$EE(\%) = \frac{TPC - FPC}{TPC} \times 100$$

C. Transmission electron microscope (TEM)

The surplus fluid was collected, using filter paper, after collection of 20 microliters of diluted samples deposited on a film-coated 200-mesh copper specimen grid for 10 minutes. After that, the grid was stained with one drop of 3% phosphotungstic acid and left to dry for three minutes. The coated grid was dried and studied at 160 Kv using a TEM microscope (JEM-2100 Electron Microscope) [16].

Production of yoghurt powder fortified with RBPL

Fresh pasteurized low-fat milk was injected by 3% (w/v) starter culture (*S. thermophilus* and *Lb. delburkii* ssp. *Bulgarius*) for production of yoghurt[17]. Yogurt samples were separated into five groups: control samples (C). Fortified sample with 1, 2, 3 and 4% of RBP-loaded-liposome marked as T1, T2, T3 and T4 respectively. Yogurt samples were preserved at -18°C for 24 hours prior to get freeze-dried in a vacuum freeze dryer (Christ, Alpha 1-2 LD plus, Osterode, Germany) at -52°C for 48 hr at a pressure of less than 0.1 mPa. The dried powder was stored at 25 °C in sterile polyethylene bags

Characterization of yoghurt powder

A- Moisture content and production yield

The production of yield (%) was calculated based on the weight ratio between the fresh yoghurt and the obtained powder from freeze-dryer [18].

B. Solubility, wettability and Bulk density

Water solubility index (WSI) was calculated according to the following formula $WSI = (\text{dried supernatant weight}) / (\text{Initial sample weight})$ [19].

Wettability of yoghurt powder was determined. 5 g of every sample was placed in 50 ml of water and the time taken to be wet was recorded [20].

The bulk density of yoghurt powder was calculated. In the same time the reconstitution of yoghurt powder was done by adding the lost water during the freeze drying process [21].

Characterizations of reconstituted yoghurt

a. Apparent viscosity

A Brook field viscometer (Brookfield Model-LV; Brookfield Engineering Laboratory, Stoughton, USA) was used to evaluate the viscosity of the reconstituted yoghurt samples [22].

b. Water holding capacity

The water holding capacity (WHC) was calculated. Twenty five g of yoghurt sample (YS) was centrifuged for 10 min at 5000 g. The whey (SW) was separated and weighed in g, and the WHC was determined as
$$WHC(\%) = \frac{YS-SW}{YS} \times 100$$

[23].

Animal Experiment

Adult 30 female Sprague Dawely rats were obtained from the animal breeding house, NRC Cairo, Egypt. The animals were kept in stainless steel cages under 12 h light/dark cycle at 25 °C. Water and feed were ad libitum. Normal basic and high fat diets (HFD) were formulated (table1) [24-25]. The experiment's protocol was approved by the Institutional Animal Care and Use Committee guidelines, NRC, (approval# 17100525/6/30/2013). Animals were divided into 3 groups (10 each), control negative group received basic commercial diet (C), the second

Table (1) Diet Formulation

Ingredients	Balanced diet (gm)*	MetS diet**
Casein	12	12
Safflower oil	10	-
Refined palm oil	-	10
Coconut oil	-	15
Sucrose	23	38
Starch	45.5	19
Vitamin mix	1	1
Mineral mix	3.5	3.5
Cellulose	5	-
Cholesterol	-	1
Bile salts	-	0.25

* Balanced diet was prepared [24]. ** Metabolic Syndrome induction diet was prepared [25].

Histopathological examination

The paraffin embedded blocks were prepared from tissue specimens (liver, kidneys, heart and ovaries), sectioned and stained with Hematoxylin and Eosin for histopathological examination [26]. Histopathological alterations were recorded and scored (0, 1, 2 and 3) as

group received HFD high carbohydrates to induce metabolic syndrome model (MetS group) (table1). The last group (RBPL) received Red beet peels loaded liposome in dose of (300mg /kg) beside HFD. After 2 months, blood samples were collected by retro-orbital puncture method under inhalation of ether anesthesia. Blood glucose was estimated then plasma was separated and kept -20°C till analysis of serum cholesterol, low and high density lipoprotein (LDL), (HDL), triglyceride (TG), total lipids, (malondaldehyde) MDA, catalase, total antioxidant, gamma glutamyl transeferase (GGT), urea, creatinine, zinc, phosphorous, leptin, insulin, T3, Thyroid stimulating hormone (TSH), insulin growth factor (IGF) and irisin using kits from Biodiagnostic, Egypt and sunlong biotech China. The whole body weight (BW) was recorded then after dissection, the liver, kidney, heart, body fat (BF) and ovaries were weighed and preserved in formalin 10% for histopathology, morphometry and immunohistochemistry study of Caspas-3 and iNOS markers. Body fat were collected to estimate the adiposity index (ADI) which was calculated as $ADI = BF / (BW - BF) \times 100$. Basic and High fat high carbohydrate diet were prepared according to table (1).

no changes, mild (<30%), moderate (<30% – 50%) and severe (>50%) respectively [27].

Histomorphometry for hepatic steatosis

The quantitative analysis of liver steatosis was based on automated counting using Image J 1.52 p software (Wayne Rasband, National Institutes of Health, U.S.A.). Five tissue sections from each group were examined. Automated counting was analyzed in 10 microscopic fields per each section under x 200-power microscopic field [28].

Histomorphometric studies of ovaries

The number of different follicles and follicular cysts from three sections of each ovary / rat (n=10) were counted microscopically using TS View version 6.2.4.5 software [29].

Immunohistochemistry

The tissue sections from liver, kidneys, heart and ovaries were deparaffinized in xylene and rehydrated in different grades of alcohol. The antigen retrieval was done by pretreating the sections with citrate buffer of pH 6 for 20 min. Sections were incubated with rabbit polyclonal anti-caspase-3 antibody at a concentration of 1:1000 (ab4051; Abcam, Cambridge, UK), and rabbit polyclonal anti-iNOS antibody at a

concentration of 1:100 (ab15323; Abcam, Cambridge, UK) for two hours in a humidified chamber. The sections were incubated with goat anti-rabbit IgG H&L (HRP) (ab205718; Abcam, Cambridge, UK). 3, 3'-diaminobenzidine tetrahydrochloride (DAB, Sigma) was used as a chromogen. Finally, the slides were counterstained with haematoxylin and mounted with DPX. The negative control slides were prepared by replacing primary antibodies using PBS [30]. The quantitative immune-reactivity of caspase-3 and iNOS was evaluated in five tissue sections in each group. 10 microscopic fields were examined per each section under high-power microscopic field (x 400). The percentage of positively stained cells (%) was estimated by color deconvolution image J 1.52 p software (Wayne Rasband, National Institutes of Health, and U.S.A.) [31].

Statistical analysis

The Duncan test was used to analyze the results. SPSS software was used for statistical analysis, and a value of $p < 0.05$ was considered statistically significant.

samples	SD (nm)	PDI	ζ -potential (mV)	Efficiency (%)
F1	118.20±2.35	0.26±0.01	-40.40±2.68	54.26±2.38
F2	115.00±3.28	0.26±0.01	-40.80±1.58	72.60±3.45
F3	119.60±4.25	0.27±0.02	-38.60±2.36	87.00±2.36
F4	113.20±1.23	0.31±0.01	-38.40±1.12	90.14±4.36
F5	108.80±1.98	0.24±0.02	-38.50±0.98	90.94±3.15

Table (2) Size distribution, polydispersity index, ζ -potential and encapsulation efficiency of RBP-loaded liposomes.

The current study showed that liposomes with 0.2, 0.4, 0.6, 0.8, and 1% RBPL had ζ -potential values of -40.4, -40.8, -38.6, -38.4, and -38.5 mV, respectively table (2). The inclusion of phosphatidic acid derived from phosphatidylcholine, which is a component of lecithin employed in liposome formation, could explain the negative ζ -potential values. The results were consistent with previous study showed that the presence of soyllecithin created the negative charged particles [11, 33]. ζ -potential varies depending on the phospholipid structure of every lecithin type. In the current study Phosphatidylcholine a zwitterionic phospholipid or zero load, was employed, with a positive (choline) and a negative (phosphate) group [34]. The magnitude of the ζ -potential of a colloidal system is linked to its physical stability. If all particles

2. Results and discussion

The total content of phenolic compounds in extract powder of red beet was 436.21±5.14 mg of Catechin equivalent per ml and the total antioxidant (DPPH%) activity was 89.51±1.26%. previous studies found that red beet peel (RBP) was more rich in phenolic and antioxidant compounds than the red beet core. Such compounds like gallic acid and betalin counteracted the inflammatory processes associated with MetS [3, 7].

RBPL characterization (Size distribution, polydispersity index and ζ -potential) (table 2) results showed that RBPL had a small particle size ranged from 108 to 118 nm most of particles were around 100 nm in size. Combining phenolic extracts to liposomes slightly increased the size distribution of the entire liposome population. Previous studies reported the same findings [32].

in a solution have a large ζ -potential (negative or positive), they repulse each other and reduce the probability to form aggregations. Earlier study stated that when the particles of ζ -potential was greater than 30 mV they were regarded as physically stable [35]. This may explain the physical stability of liposome in the current study (table 2).

Transmission electron microscopy (TEM) was used to investigate the morphology of the liposomes, which revealed spherical vesicles in all images (Fig. 1). Furthermore, the size distribution was diverse, with some clearly visible aggregates which were consistent with the observed polydispersity index (PDI) (table 2). The current findings were consistent with previous studies which found that utilized liposomes in the

encapsulation of phenolic extracts had a size distribution greater than 200 nm [36].

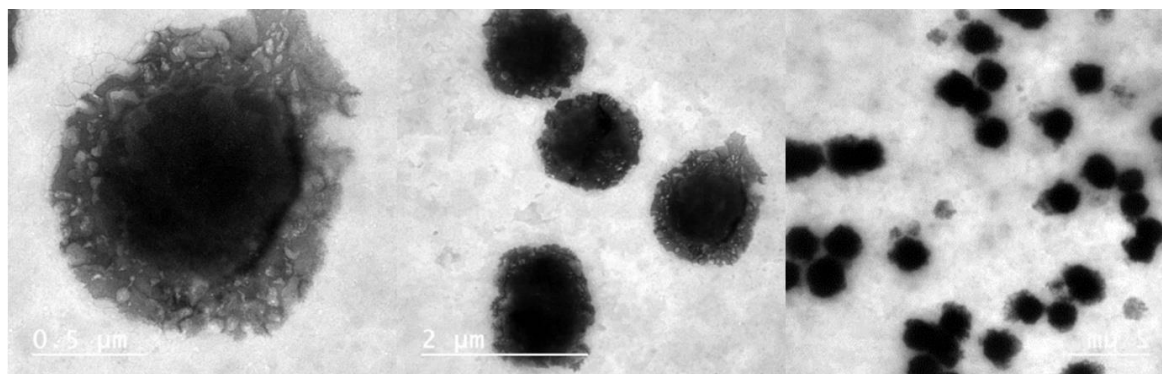


Figure 1. TEM micrograph of RBP-loaded liposome obtained at a scale of 0.5 and 2 μm .

Physical and functional properties of yoghurt powder physical characteristics of yoghurt powders after freeze-drying (Table 3) showed that the inclusion of RBPL increased the moisture content from 5.19 to 9.12 % and yield 11.01 to 12.55% for control and T₄ of yoghurt powders ($p < 0.05$), respectively. The liposomes hold more moisture during the freeze-drying process similar to earlier studies [37, 18, and 12].

The bulk density of yoghurt powders was significantly increased when RBPL were added, with findings ranging from 0.53 to 0.32 g cm^{-3} for control and T₄ ($p < 0.05$), respectively. Earlier studies showed similar bulk density (538 g cm^{-3}) when using spray [38], while lower density was shown in freeze drying (0.22 g cm^{-3}) [39].

Table (3) Physical and functional properties of yoghurt powders and reconstituted yoghurts

Values are the mean \pm SD; values with different lowercase superscript letters in the same column are significant ($p < 0.05$). control (C), yoghurt sample with 1% RBP-loaded-liposome (T₁), yoghurt sample with 2% RBP-loaded-liposome (T₂), yoghurt sample with 3% RBP-loaded-liposome (T₃), and yoghurt sample with 4% RBP-loaded-liposome (T₄).

No.	Yoghurt powder					Reconstituted yoghurt	
	Moisture (%)	Yield (%)	Bulk density (g cm^{-3})	Solubility (%)	Wettability (s)	Viscosity (Pa.s)	WHC (%)
C	5.19 ^c \pm 0.10	11.01 ^b \pm 0.93	0.32 ^b \pm 0.02	76.81 ^d \pm 0.63	29.50 ^a \pm 0.71	8.28 ^a \pm 0.38	58.20 ^a \pm 0.28
T ₁	6.37 ^d \pm 0.08	11.66 ^{ab} \pm 0.05	0.33 ^b \pm 0.03	79.78 ^c \pm 0.33	29.00 ^a \pm 1.41	8.17 ^{ab} \pm 0.08	55.60 ^b \pm 0.57
T ₂	7.61 ^c \pm 0.16	11.49 ^{ab} \pm 0.45	0.40 ^b \pm 0.05	83.97 ^b \pm 1.16	27.50 ^{ab} \pm 0.71	7.72 ^b \pm 0.31	51.80 ^c \pm 0.28
T ₃	8.63 ^b \pm 0.11	12.07 ^{ab} \pm 0.39	0.41 ^b \pm 0.03	85.40 ^{ab} \pm 0.37	25.50 ^b \pm 0.71	5.92 ^c \pm 0.11	51.40 ^c \pm 0.85
T ₄	9.21 ^a \pm 0.13	12.55 ^{ab} \pm 0.40	0.53 ^a \pm 0.03	86.77 ^a \pm 0.42	22.00 ^c \pm 1.41	5.17 ^d \pm 0.04	51.00 ^c \pm 1.41

The yoghurt powders' solubility and wettability characteristics, the addition of RBP-loaded liposomes in production of yoghurt powders enhanced the solubility of the yoghurt powders and reduced their wetting time table 3. These findings are consistent with another study [40]. The viscosity and water holding capacity (WHC) of reconstituted yoghurt samples made from freeze-dried powdered showed that when adding RBPL to yoghurt RBPL caused reduction of the viscosity values ($p <$

0.05)(table 3). This irreversible deterioration of the structure of the yoghurt gel network was seen in other studies [41-42].

Animal experiment results:

In the current study Analysis of plasma biochemical parameters (table 4) showed significant increase in glucose, total cholesterol (TC), low density lipoprotein (LDL), triglyceride (TG), total lipids, gamma glutamyl transferase (GGT), leptin, irisin, malondialdehyde (MDA) and urea in the group of rats with induced metabolic syndrome (MetS), if

compared to normal animals. In the same time this group showed significant decrease in high density lipoprotein (HDL), albumin, catalase, total antioxidant, TSH, T3, insulin, IGF phosphorus and zinc if compared to normal control group. Administration of red beet peel liposomes took mostly all the disrupted values back towards normal.

The elevated blood glucose in MetS group was sequelae of the continuous challenge with high-fat high CHO diet that resulted in loss of glucose homeostasis in blood. Red Beet was mentioned in earlier studies for its bioactive potential in improving blood glucose by inhibition of carbohydrate digestion and glucose absorption in the intestine, and modulated glucose release from the liver [43-44]. Dyslipidemia (elevation of TC, LDL, TG and low levels of HDL-cholesterol) was since long related to metabolic syndrome [45-46]. These findings coincide with the current study results. The saturated fats present in the high-fat diet are responsible for the increased lipid profile indices

(table 4), hepatic steatosis shown in morphometry study and elevated liver enzymes such as γ -GT [47-48]. Previous studies showed that RB corrected the abnormalities of lipid profile markers [49] as it is rich in betalains that reduce homocysteine concentration and regulate the vascular homeostasis [50]. These results were confirmed by histopathological picture (figs 2 & 3) and lesion scoring (table 7) of liver. The hepatocytes in current study showed severe macro and microvesicular steatosis (fig. 2 b) and necrosis with mononuclear inflammatory cells infiltration (fig. 2 c) with portal fibrosis (fig. 2 d) in MetS group compared to normal control group (fig 2 a) those were the same as in previous studies [51-52].

Histo-morphometric measures (table 6) showed marked elevated number of vacuolated hepatocytes in MetS group. RBPL treated group showed lower number of vacuolated hepatocytes and less steatosis score and milder edema in portal area (figs. 3 a&b and table 6). This was seen in other previous studies [51-52].

Table (4) Effect of RBPL on plasma biochemistry of MeS induced female rats

Parameters	Normal Control	MetS group	RBPL
Glucose (mg/dL)	98.8 ± 0.99 ^a	149.7 ± 0.81 ^b	111 ± 3.7 ^c
Total cholesterol (mg/dL)	100 ± 2.81 ^a	341.6 ± 6.83 ^b	187 ± 10.66 ^c
HDL (mg/dL)	47.2 ± 0.91 ^a	39.4 ± 1.04 ^b	32.8 ± 0.98 ^c
LDL (mg/dL)	39.9 ± 0.84 ^a	240.8 ± 2.45 ^b	77.6 ± 3.59 ^c
Triglycerides (mg/dL)	78.4 ± 1.11 ^a	107 ± 1.25 ^b	93.3 ± 0.94 ^c
γ -GT (g/dL)	83 ± 0.6 ^a	105.4 ± 0.24 ^b	57.6 ± 0.1 ^c
Albumin (g/dL)	2.51 ± 0.06 ^a	2.5 ± 0.01 ^a	2.6 ± 0.01 ^a
Leptin (ng/ml)	10.24 ± 0.02 ^a	11.30 ± 0.13 ^b	10.40 ± 0.04 ^c
Irisin (ng/ml)	15.53 ± 0.17 ^a	17.89 ± 0.18 ^b	11.11 ± 0.18 ^c
Catalase (mg/dL)	59.98 ± 0.90 ^a	44.56 ± 0.44 ^b	49.29 ± 0.85 ^c
MDA (mg/dL)	19 ± 0.11 ^a	29 ± 0.16 ^b	10 ± 0.13 ^c
Creatinine (mg/dL)	0.68 ± 0.01 ^a	0.6 ± 0.01 ^a	0.7 ± 0.01 ^a
Urea (mg/dL)	32 ± 0.10 ^a	38.5 ± 0.24 ^b	27 ± 0.22 ^c
Phosphorus (mg/dL)	12.88 ± 0.21 ^a	9.75 ± 0.06 ^b	7.92 ± 0.36 ^c
Zinc (μ g/dL)	178.9 ± 2.93 ^a	121.6 ± 1.96 ^b	112.1 ± 1.92 ^c
IGF-1 ng/ml	588.81 ± 9.84 ^a	429.17 ± 4.16 ^a	550.86 ± 20.67 ^c
Insulin μ U/ml	17.10 ± 0.33 ^a	9.89 ± 0.15 ^b	12.40 ± 0.34 ^c
Total lipids mg/dL	317.3 ± 20.41 ^a	548.49 ± 22.13 ^b	454.77 ± 31.30 ^c
T3 (ng/ml)	11.67 ± 0.72 ^a	11.09 ± 0.18 ^b	11.83 ± 0.17 ^a
TSH (ng/ml)	2.04 ± 0.04 ^a	1.50 ± 0.17 ^b	1.20 ± 0.06 ^b
Total antioxidant (mM/L)	2.13 ± 0.03 ^a	1.43 ± 0.04 ^b	1.99 ± 0.11 ^c

Different superscripts within rows mean significance ($p < 0.05$).

Table (5) Effect of RBPL on organ body fat weight and ADI in experiment groups

	Control	MetS	RBPL
Body fat	6.6 ± 0.25 ^a	12.1 ± 0.62 ^b	10.6 ± 0.5 ^c
ADI*	7.53±0.59 ^c	22.25± 0.7 ^a	21.86± 0.7 ^a
Heart (gm)	0.77± 0.03 ^c	0.93 ±0.05 ^b	0.88 ±0.05 ^{bc}
Liver (gm)	6.1± 0.49 ^{ab}	8.5± 0.51 ^a	9.18± 0.19 ^a

*ADI = BF (BW-BF) /100). Different superscripts within rows mean significance (p<0.05).

Photomicrograph of myocardium and aorta (fig 2j) showed hyaline degeneration of myocytes, and thickened aortic wall with injury of endothelial lining in MetS group. Earlier studies coincide with our results [53]. The arterial stiffness and thickening in obesity was attributed to hypertension, cardiovascular complication due to oxidative stress and inflammatory reaction [54]. RBPL group (fig 3 d) showed normal myocytes and moderate aortic thickening. This may be due to hypoglycemic, antioxidant, and anti-inflammatory effects of red beet [55]. The current study showed elevated Leptin and Irisin hormones level in plasma of MetS group (table 4). Earlier study reported the high leptin level in association to metabolic syndrome and obesity [56]. Its concentration in the blood reflects total body fat as signaling information to the brain and stimulates hypothalamus to regulate food intake and increase energy expenditure [57]. Increased Bf and ADI were noticed in this study with elevation of leptin, total lipids and irisin. Increased level of blood irisin positively correlates with energy expenditure; ameliorating obesity, and glucose homeostasis. RBPL administration lowered both BF and ADI (table 5) and the levels of leptin, total lipids and irisin back toward normal control levels table (4). This may be due to presence of some pharmaceutical compounds like betalain that reduce adiposity, improve energy homeostasis and glucose tolerance in rats [50, 58]. These evidences showed that Leptin and Irisin levels may be used as an independent predictor of metabolic syndrome, insulin resistance, glucose imbalance, fat mass and the high risk of cardiovascular disease [59]. The current results showed higher oxidative marker (MDA) and lower antioxidant (catalase, total antioxidants) levels in MetS compared to control group (table 4). The high fat diet causes depletion of antioxidant markers leading to increased superoxide anion and hydrogen peroxide in biological systems, which in turn generate hydroxyl radicals resulting in lipid peroxidation [60].

Immunohistochemical results (table 8, figs 4&5) of Caspase-3 and iNOS in liver, kidney, myocardium and aorta revealed strong expression of both markers in MetS group, suggesting the pathogenesis of HFD-mediated cell injury, apoptosis (Caspase-3) and inflammation and oxidative stress (iNOS). RBPL administration ameliorates this oxidative stress presented by less expression levels of both markers (table 8). This effect may be due to hypoglycemic, insulin-sensitizing, antioxidant and anti-inflammatory effects of red beet [55] (figs 4&5). RBPL is high source of polyphenols and flavonoids, which may enhance the antioxidant defense in tissues under oxidative stress [61].

Histopathology of Kidney of MetS treated with RBPL group showed renal tubular necrosis, interstitial fibrosis, inflammation and heavy infiltration of adipose tissue in renal capsule (figs. 2 f, g & h) indicating dysfunctional reabsorption due to HFD. Also, there was congestion of interstitial blood vessels in MetS group when compared with normal control (fig 2 e) [62]. RBPL group showed a significant decrease of blood urea towards normal levels and improved histopathological picture in kidney, as it protects renal tissue by its antioxidant activity leading to the improvement of kidney function (Fig. 3c) [63].

Phosphorus and zinc showed significant decrease in MetS group when compared with normal control. Low zinc level is associated with increased oxidative stress and generation of inflammatory status than in healthy people [64-65].

Organ and fat weight showed significant increase in weights of heart, liver fat and ADI in MetS group, when compared with normal animal control. RBPL significantly lowered body fat weight towards normal Table (5), previous studies showed similar results [52].

In the current study, the group of animals fed on high fat diet MetS group showed high blood sugar, hyperlipidemia and low antioxidant concentration (table 4) accompanied with significant decrease in the number of mature graffian follicles and high prevalence of follicular cysts (fig. 6 and table 6).

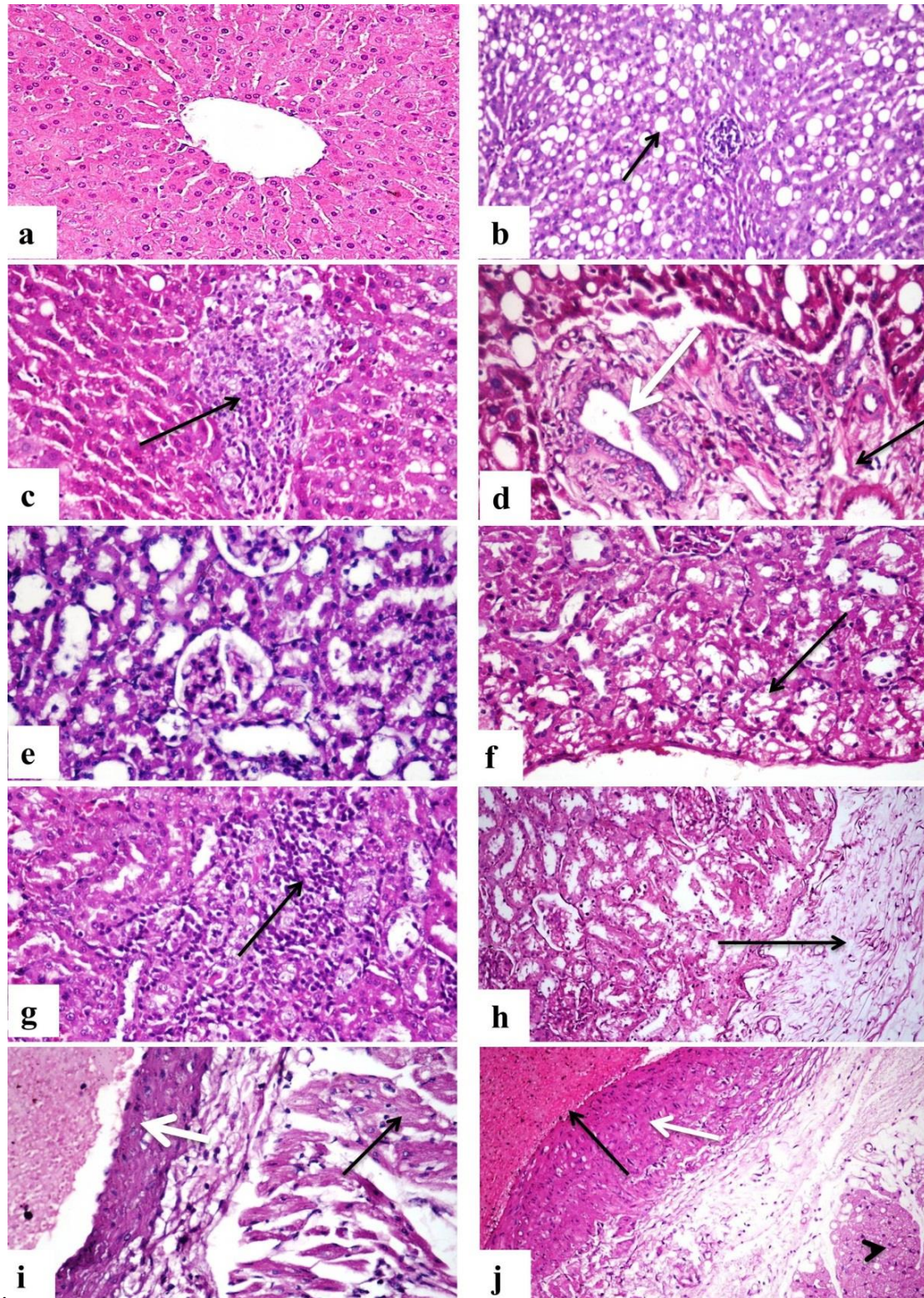


Figure 2. Photomicrograph, female rat, liver, kidney and heart. (a) liver, control group (H&EX400). (b) liver, MetS group showing diffuse macrovesicular steatosis in hepatocytes (arrow) (H&EX200). (c) liver, MetS group showing necrosis of hepatocytes with infiltration with mononuclear cells (arrow) (H&EX400). (d) liver, MetS group showing portal fibrosis (black arrow), bile duct hyperplasia (white arrow) (H&EX400). (e) kidney, control group (H&EX400). (f) kidney of MetS showing vacuolar degeneration and necrosis of renal tubules (arrow) (H&EX400). (g) kidney of MetS showing interstitial fibrosis with infiltration of mononuclear cells (arrow) (H&EX400). (h) kidney of MetS showing adipose tissue infiltration in renal capsule (arrow) (H&EX200). (i) myocardium (black arrow) and aorta (white arrow) of control group (H&EX400). (j) myocardium of MetS showing hyaline degeneration of myocytes (arrowhead), aorta showing thickening of its wall (white arrow) with injury of endothelial lining (black arrow) (H&EX400).

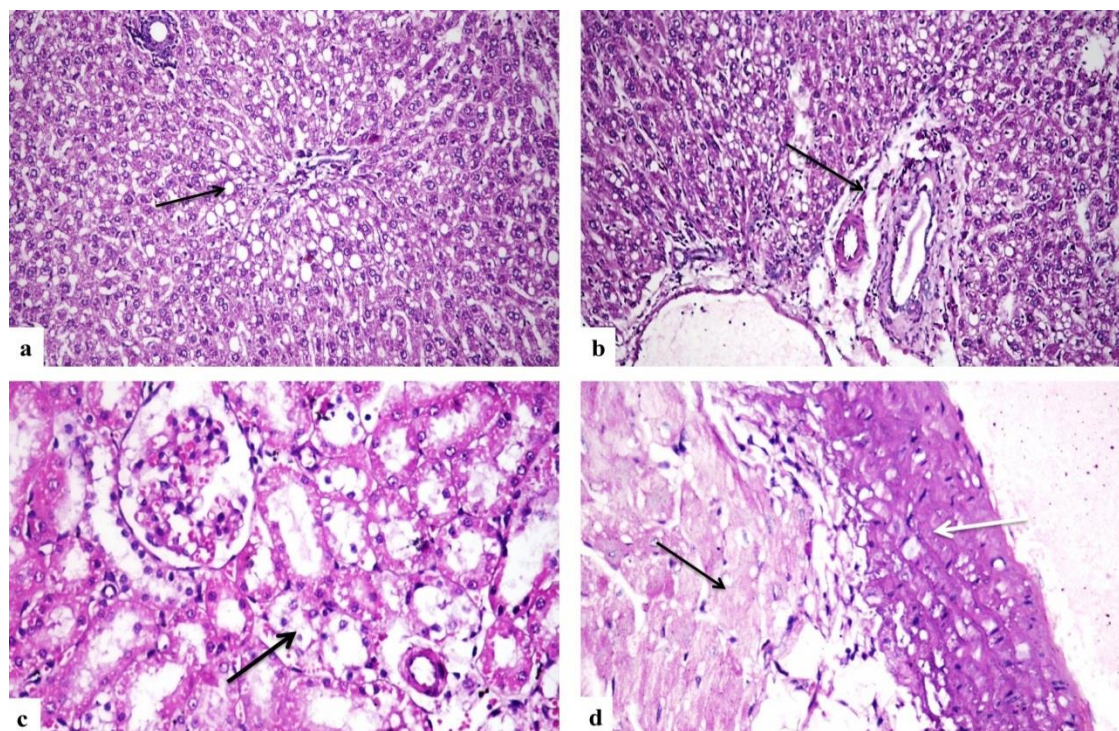


Figure 3. Photomicrograph of MetS+RB treated group (a) liver showing focal macro and microvesicular steatosis in few hepatocytes (arrow) (H&EX200). (b) liver showing mild edema in portal area (arrow)(H&EX200). (c) kidney showing moderate vacuolar degeneration of renal tubular lining epithelium (arrow) (H&EX400). (d) heart showing nearly normal myocytes (black arrow) and moderate aortic thickening (white arrow) (H&EX400).

The immunostaining expression of caspase-3 (apoptotic marker) and iNOS (pro-inflammatory and oxidative stress marker) % area in ovaries (table 8, fig 8 b) revealed strong expression of both markers in granulosa and stromal cells in the same group of animals. Hyperglycemia leads to advanced glycation end-products that produce reactive oxygen species [66] which cause damaged cell membranes, lipid peroxidation, apoptosis of granulosa cells and stop oocyte maturation leading to subsequent follicular atresia [4-5]. Other authors referred the condition to the effect of hyperglycemia on thecal angiogenesis, this vascular network which originates from theca interna, surrounding the granulosa cells to drive nutrients to follicular fluid for the development of the ovum and follicle [67-68]. The chronic exposure to hyperglycemia significantly suppresses vascular endothelial growth factor which has a critical role in the process of thecal angiogenesis [69-70].

The current study showed that the group of animals fed on MetS group revealed significant decrease in TSH, estrogen, insulin and IGF1 table (4). Previous studies recorded that patients with T2DM presented with long-term absolute or relative insulin deficiency, reduced thyroid iodine uptake and poor thyroid function [71]. Insulin acts as a co-gonadotropin with LH [72] so that, insulin resistance, low estrogen,

hyper-androgenism results in oligo-ovulation/ anovulation, and multiple cysts formation in obese individuals [73].

Obesity may interfere with follicular development through mammalian target of rapamycin (mTOR), which is a serine/threonine kinase that regulates the cell growth and proliferation in response to stress, nutrients, and growth factors [73]. Consequently, over activation of ovarian follicles might accelerate the rate of follicle loss via promoting follicle apoptosis, so obesity leads to a marked increase in the number of atretic follicles through triggering follicular apoptosis [73]. Which was shown in current study by increased expression of Caspase-3 (apoptotic marker).

The present study showed that RBPL group showed decreased level of glucose and total lipids and in the same time elevated level of antioxidants, insulin, IGF and estrogen hormones table (4). Histological findings (fig 7 and table 6) showed increased number of mature follicles and lower incidence of follicular cysts in RBPL group. These findings may be due to the higher content of phenolic compounds and higher antioxidant power in RB. This explanation was proved by the lower immune-expression of Caspase-3 and iNOS in ovarian tissue (fig. 8 c, table 8) in RBPL group that means reduced oxidative stress and apoptotic process

which previously resulted from hyperglycemia and was demonstrated in MetS group.

MetS group showed increased numbers of corpora lutea (fig. 6d). As obesity causes elevation of the levels of free fatty acids exceeding the lipid storage capacity of the adipose tissue, free fatty acids begin to accumulate in the organs “ectopic lipid deposition”, Which precipitates Ovarian dysfunction as a result of disordered fatty acid metabolism [74]. There was also an evidence of formation of follicular cyst (fig 6 c & e, table 6). Insulin resistance as a complication of MetS resulted on development of polycystic ovary, through

development of hyper-androgenism, oligo-ovulation/ anovulation, and multiple cysts in obese individuals [73]. These changes are caused mainly due ovarian androgen synthesis, hyper-insulinemia [72]. RBPL treated group showed moderate improvement in number of ovarian follicles with decreased formation of follicular cysts (fig. 7, table 6). Many health benefits of beetroot (*Beta vulgaris* L.) have been recorded in several studies, including antioxidant, anti-inflammatory, anti-diabetic, nephroprotective, hepatoprotective and hypoglycemic potential [75].

Table (6) Evaluation of macro and microvesicular steatosis, ovarian follicles and ovarian cysts in different treated groups

Groups	CTRL	MetS	MetS+RBPL
No. of vacuolated hepatocytes	0	170± 8.34 ^b	95± 6.91 ^a
No. of ovarian follicles	19.25±2.53 ^b	4.75±1.82 ^a	8.5±1.71 ^c
No. of follicular cysts	0	5.6±1.32 ^b	2.6±0.88 ^c

Data was expressed as mean ± SEM, (n = 10). Different letters in the same column were significantly different at (p ≤ 0.05).

Table (7) Scoring of histopathological alterations in liver, kidneys and heart of all groups

Lesions	CTRL	MetS	MetS+RBPL
LIVER:			
- Steatosis	0	3	2
- Necrosis and mononuclear inflammatory cells infiltration between hepatocytes	0	2	1
- Portal fibrosis	0	3	2
- Hyperplasia of bile ducts	0	2	1
KIDNEYS			
- Infiltration of capsule with fat cells	0	3	2
- Interstitial fibrosis	0	2	1
- Interstitial mononuclear inflammatory cells infiltration	0	2	1
- Vacuolar degeneration and necrosis of tubular lining epithelium	0	3	2
HEART			
- Necrosis of myocytes	0	2	1
- Thickening of aorta	0	3	2
- Necrosis of aortic endothelium	0	2	1

The score system was designed as: score 0 = absence of the lesion in all rats of the group (n= 5), score 1= (<30%), score 2= (<30% – 50%), score 3= (>50%).

Table (8) Area % of Caspase-3 and iNOS expression in liver, kidneys, heart and ovary of different experimental groups

	CTRL	MetS	MetS+RBPL
<u>Caspase-3</u>			
Liver	0	47.23±0.98 ^b	31.33±0.75 ^a
Kidneys	0	41.67±2.43 ^b	29.81±1.55 ^a
Myocardium	0	48.22±1.92 ^b	33.17±1.88 ^a
Aorta	0	36.23±0.39 ^b	21.99±0.73 ^a
Ovary	0	55.12±3.90 ^b	39.82±2.75 ^a
<u>iNOS</u>			
Liver	0	51.20±3.74 ^b	36.01±0.86 ^a
Kidneys	0	43.02±0.97 ^b	30.05±1.91 ^a
Myocardium	0	48.92±2.19 ^b	31.98±1.05 ^a
Aorta	0	58.34±2.12 ^b	22.09±0.39 ^a
Ovary	0	53.29±1.97 ^b	41.13±3.18 ^a

Data was expressed as mean ± SEM, (n = 10). Different letters in the same column were significantly different at ($p \leq 0.05$).

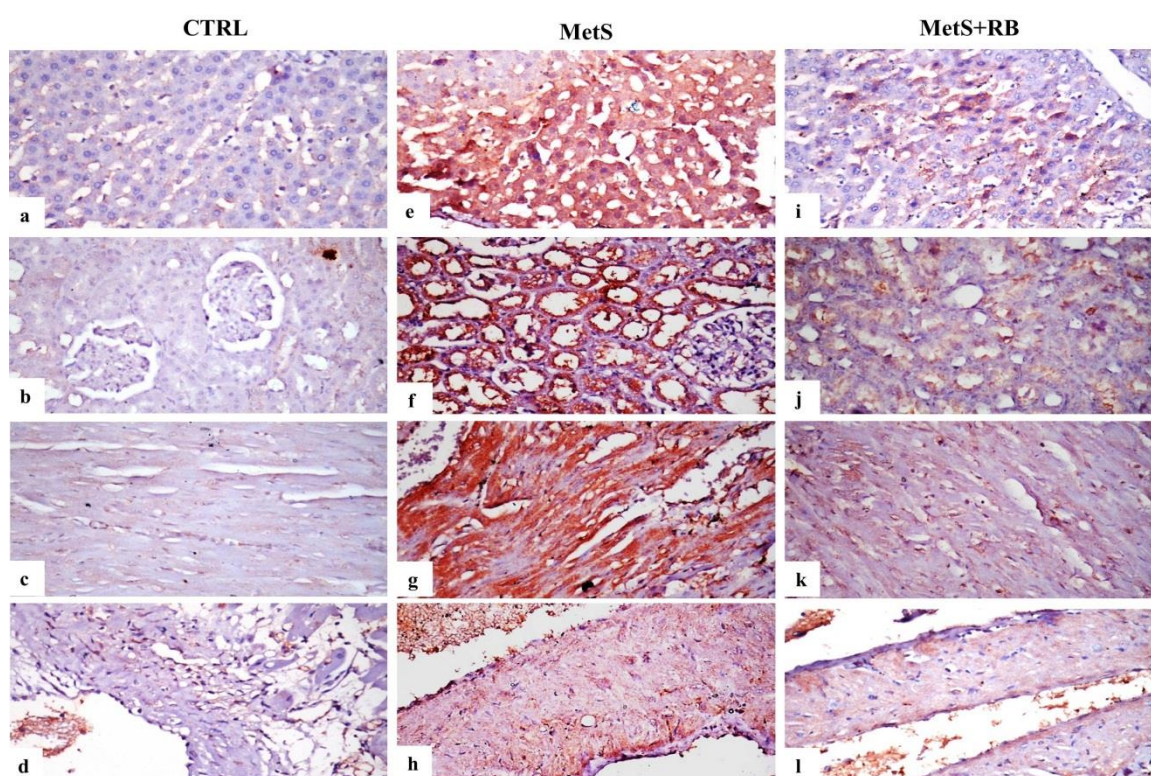


Figure 4. Immunostaining of Caspase-3, liver, kidney and heart. (a)- (d) control group: liver, kidney, myocardium and aorta respectively, showing no immune expression. (e)- (h) MetS group, liver, kidney, myocardium and aorta respectively, showing strong expression. (i)- (l) MetS+RB: liver, kidney, myocardium and aorta respectively, showing weak positive expression of Caspase-3 (Caspase-3 X400).

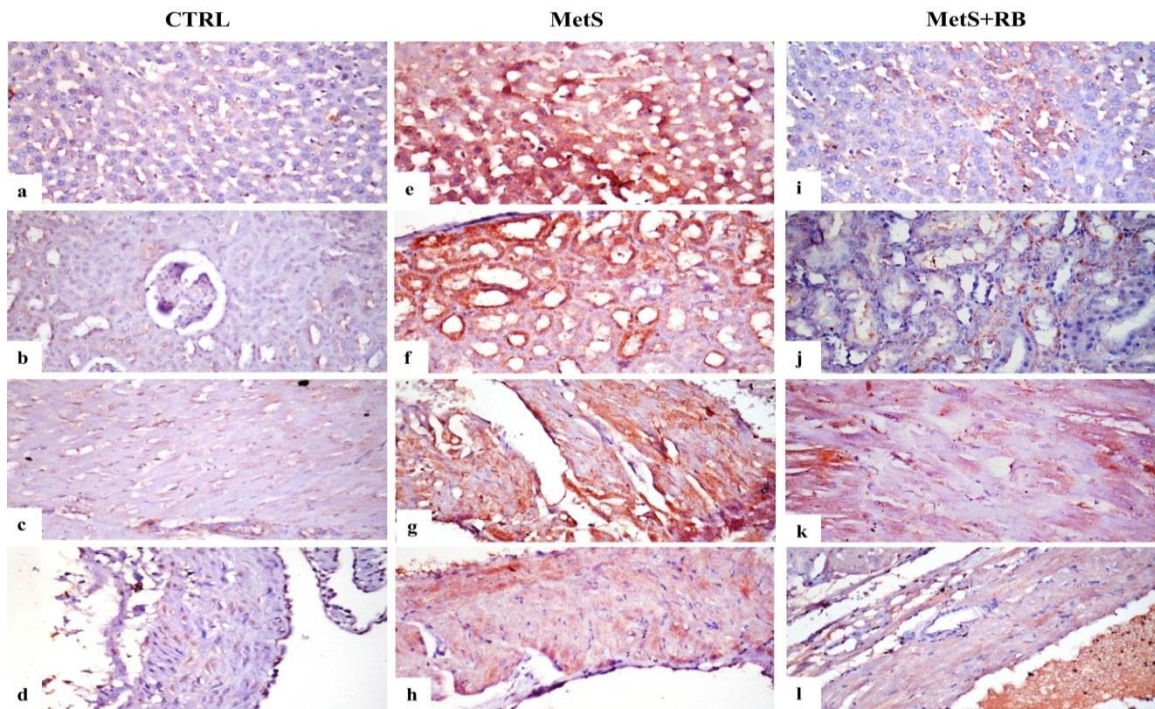


Figure 5. Immunostaining of iNOS , liver, kidney and heart. (a)- (d) control group: liver, kidney, myocardium and aorta respectively, showing no immune expression. (e)- (h) MetS group, liver, kidney, myocardium and aorta respectively, showing strong expression. (i)- (l) MetS+RB: liver, kidney, myocardium and aorta respectively, showing weak positive expression of iNOS (iNOS X400).

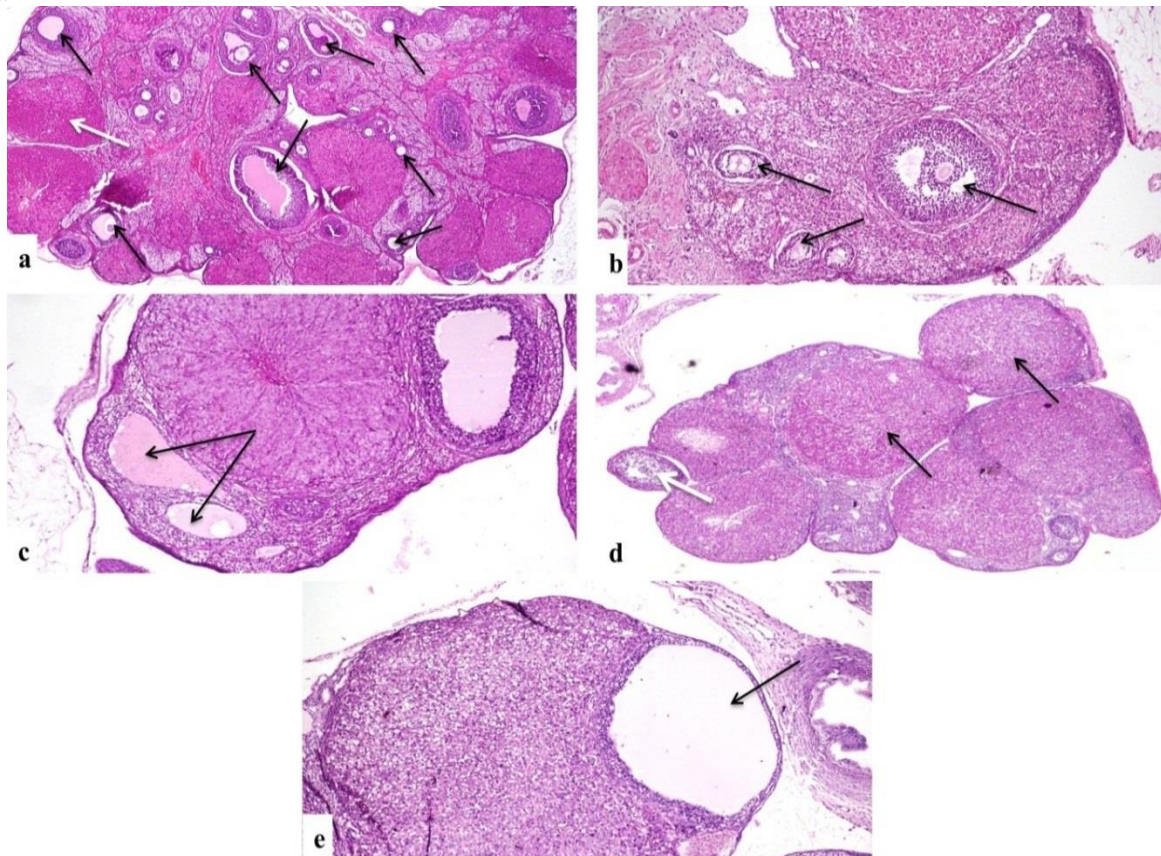


Figure 6. Photomicrograph, rat ovary. (a) control group showing large number of follicle (black arrows) and few corpora lutea (white arrow) (H&EX40). (b) HFD group showing few mature follicles (arrows) (H&EX40). (c) HFD group showing few ovarian follicles with tendency of follicles to form follicular cyst (arrows) (H&EX100). (d)HFD group showing increased proportion of corpora lutea (black arrows) with decreased mature follicles (white arrow) (H&EX40). (e) HFD group showing formation of follicular cyst with characteristic thin wall and attenuated granulosa cell lining (arrow) (H&EX40).

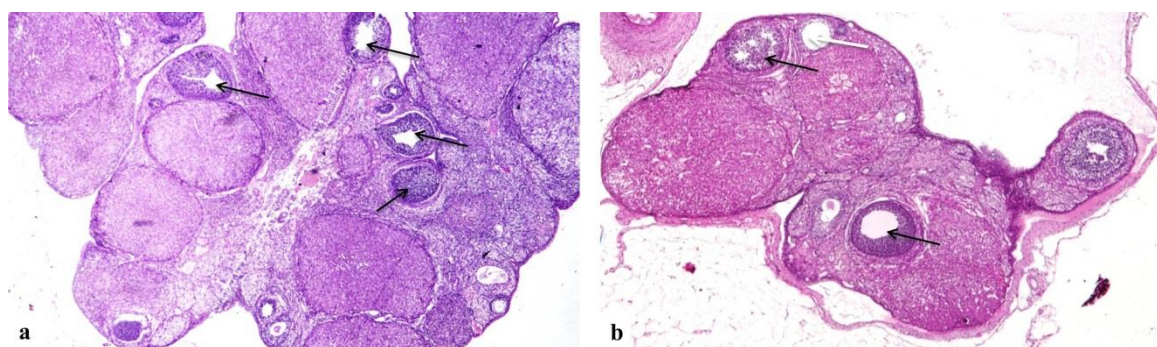


Figure 7. Photomicrograph, rat ovary, HFD+RB treated group. (a) showing relative increase in number of mature follicles (arrows). (b) notice presence of mature follicles (black arrows) with few follicular cysts (white arrow), (H&EX40).

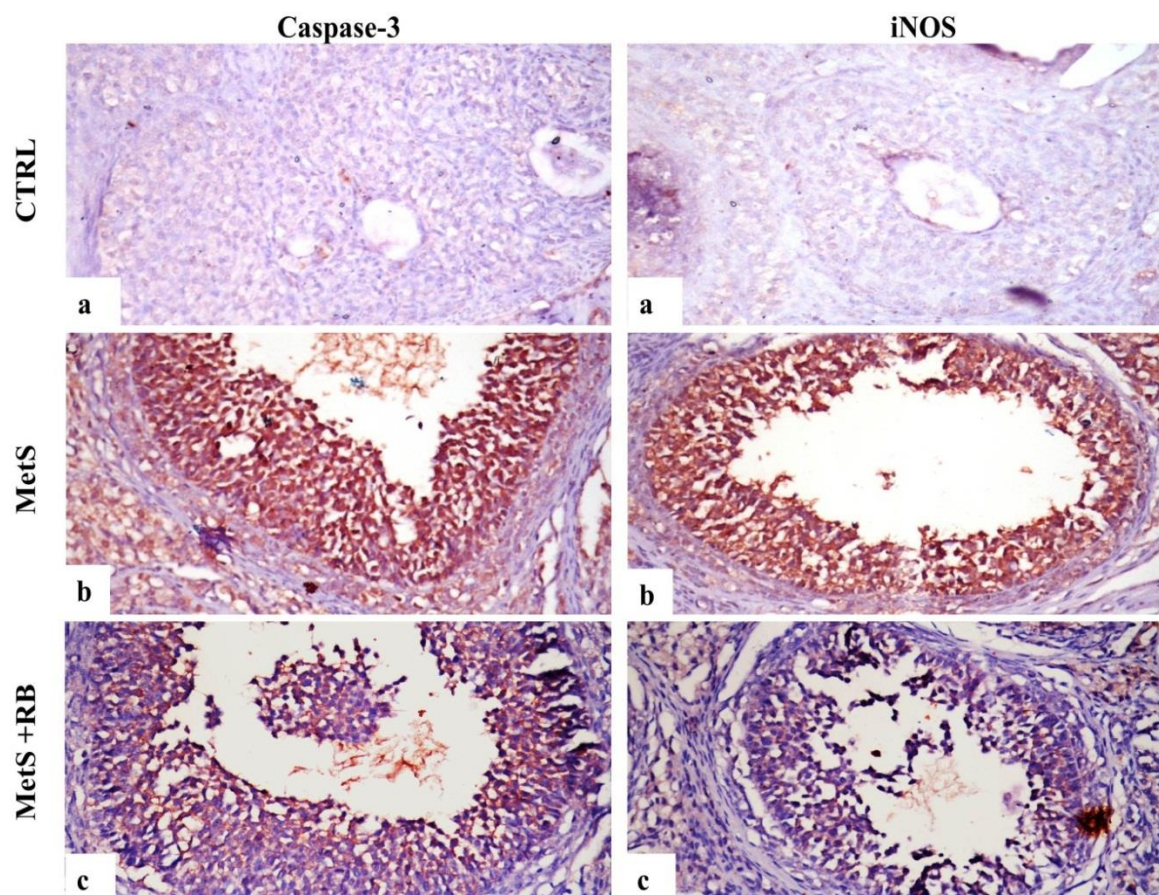


Figure 8. Immunostaining of Caspase-3 and iNOS in ovarian tissue. (a) control group showing no immune expression for both markers. (b) HFD group showing strong expression in granulosa cells and stromal cells. (c) HFD+RB treated group showing moderate expression of Caspase-3 and iNOS in granulosa cells and stromal cells. (Caspase-3 and iNOS X200).

3- Conclusions

RBPL were able to protect active phenolic compounds in red beet peel extract and helped in controlling lipid profile, glucose level and most of other biochemical parameters in MetS rat model. Histopathology and immunohistochemistry showed mild to moderate improvement of liver steatosis and ovarian function. This may need more study and longer period of treatment. Production of dried yoghurt fortified with RBPL may be innovative

3. Conflicts of interest

The work team declared that there are no conflicts of interest and all authors agreed for publication.

4. Formatting of funding sources

This research was funded by internal project from NRC number (12050250) 2019-2021.

7. Acknowledgement

All work team would like to express their thanks for NRC Egypt which funded this work through internal project No 12050210.

8. References

- [1] Tremmel, M., Gerdtham, U. G., Nilsson, P. M., & Saha, S. (2017). Economic burden of obesity: a systematic literature review. *International journal of environmental research and public health*, 14(4), 435.
- [2] Ansari-Moghaddam, A., Adineh, H. A., Zareban, I., & Farmanfarma, K. K. (2019). Prevalence of metabolic syndrome and population attributable risk for cardiovascular, stroke, and coronary heart diseases as well as myocardial infarction and all-cause mortality in middle-east: Systematic review & meta-analysis. *Obesity Medicine*, 14, 100086.
- [3] Paradiso, V. M., Castellino, M., Renna, M., Gattullo, C. E., Calasso, M., Terzano, R., & Santamaria, P. (2018). Nutritional characterization and shelf-life of packaged microgreens. *Food & function*, 9(11), 5629-5640.
- [4] Chang AS, Dale AN, Moley KH. Maternal diabetes adversely affects preovulatory oocyte maturation, development, and granulosa cell apoptosis. *Endocrinology*. 2005; 146: 2445.
- [5] Wu Y, Zhang Z, Liao X, Wang Z. High Fat Diet Triggers Cell Cycle Arrest and Excessive Apoptosis of Granulosa Cells during the Follicular Development. *Biochemical & Biophysical Research Communications*. 2015; 466: 599-605.
- [6] Kanner, J., Harel, S., & Granit, R. (2001). Betalains a new class of dietary cationized antioxidants. *Journal of Agricultural and Food chemistry*, 49(11), 5178-5185.
- [7] Angelino, D., Godos, J., Ghelfi, F., Tieri, M., Titta, L., Lafranconi, A., & Grosso, G. (2019). Fruit and vegetable consumption and health outcomes: An umbrella review of observational studies. *International Journal of Food Sciences and Nutrition*, 70(6), 652-667.
- [8] Kujala, T. S., Loponen, J. M., Klika, K. D., & Pihlaja, K. (2000). Phenolics and betacyanins in red beetroot (*Beta vulgaris*) root: Distribution and effect of cold storage on the content of total phenolics and three individual compounds. *Journal of agricultural and food chemistry*, 48(11), 5338-5342.
- [9] Liu, Y., Ji, M., Wong, M. K., Joo, K. I., & Wang, P. (2013). Enhanced therapeutic efficacy of iRGD-conjugated crosslinked multilayer liposomes for drug delivery. *BioMed research international*, 2013.
- [10] Zhou, W., Liu, W., Zou, L., Liu, W., Liu, C., Liang, R., & Chen, J. (2014). Storage stability and skin permeation of vitamin C liposomes improved by pectin coating. *Colloids and surfaces B: Biointerfaces*, 117, 330-337.
- [11] El-Said, M. M., El-Messery, T. M., & El-Din, H. M. (2018). The encapsulation of powdered doum extract in liposomes and its application in yoghurt. *Acta Scientiarum Polonorum Technologia Alimentaria*, 17(3), 235-245.
- [12] Santos, G., Nunes, T. P., Silva, M. A. A. P., Rosenthal, A., & Pagani, A. A. C. (2018). Development and acceptance of freeze-dried yogurt "powder yogurt". *International Food Research Journal* 25(3):1159-1165
- [13] El-Messery, T. M., El-Said, M. M., Salama, H. H., Mohammed, D. M., & Ros, G. (2021). Bioaccessibility of Encapsulated Mango Peel Phenolic Extract and its Application in Milk Beverage. *International Journal of Dairy Science*, 16(1), 29-40.
- [14] Naczki, M., & Shahidi, F. (1989). The effect of methanol-ammonia-water treatment on the content of phenolic acids of canola. *Food Chemistry*, 31(2), 159-164.
- [15] Brand-Williams, W., Cuvelier, M. E., & Berset, C. L. W. T. (1995). Use of a free radical method to evaluate antioxidant activity. *LWT-Food science and Technology*, 28(1), 25-30.
- [16] Saloko, S., Darmadji, P., Setiaji, B., Pranoto, Y., & Anal, A. K. (2013). Encapsulation of coconut shell liquid smoke in chitosan-maltodextrin based nanoparticles. *International Food Research Journal*, 20(3).
- [17] Haji Ghafarloo, M., Jouki, M., & Tabari, M. (2020). Production and characterization of synbiotic Doogh, a yogurt-based Iranian drink by gum arabic, ginger extract and *B. bifidum*. *Journal of Food Science and Technology*, 57(3), 1158-1166.
- [18] Jouki, M., Khazaei, N., Rezaei, F., & Taghavian-Saeid, R. (2021). Production of synbiotic freeze-dried yoghurt powder using microencapsulation and cryopreservation of *L. plantarum* in alginate-skim milk microcapsules. *International Dairy Journal*, 122, 105133.
- [19] Jafari, S. M., Ghalenoei, M. G., & Dehnad, D. (2017). Influence of spray drying on water solubility index, apparent density, and anthocyanin content of pomegranate juice powder. *Powder technology*, 311, 59-65.
- [20] Koç, B., Yilmazer, M. S., Balkır, P., & Ertekin, F. K. (2010). Moisture sorption isotherms and storage stability of spray-dried yogurt powder. *Drying Technology*, 28(6), 816-822.
- [21] Jinapong, N., Suphantharika, M., & Jamnong, P. (2008). Production of instant soymilk powders by ultrafiltration, spray drying and fluidized bed agglomeration. *Journal of food engineering*, 84(2), 194-205.
- [22] Jafari, S., Jouki, M., & Soltani, M. (2021). Modification of physicochemical, structural, rheological, and organoleptic properties of sweetened condensed milk by maltodextrin, fructose, and lactose. *Journal of Food Measurement and Characterization*, 15(4), 3800-3810.
- [23] Arslan, S., & Özel, S. (2012). Some properties of stirred yoghurt made with processed grape seed powder, carrot juice or a mixture of grape seed powder and carrot juice. *Milchwissenschaft*, 67(3), 281-285.
- [24] Reeves, P. G., Nielsen, F. H., & Fahey Jr, G. C. (1993). AIN-93 purified diets for laboratory rodents: final report

- of the American Institute of Nutrition ad hoc writing committee on the reformulation of the AIN-76A rodent diet.
- [25] Panchal, S. K., & Brown, L. (2010). Rodent models for metabolic syndrome research. *Journal of Biomedicine and Biotechnology*, 2011.
- [26] Bancroft, J. D., & Gamble, M. (Eds.). (2008). Theory and practice of histological techniques. Elsevier health sciences.
- [27] Korany, R. M., Ahmed, K. S., Halawany, H. A. and Ahmed, K. A. 2019. Effect of long-term arsenic exposure on female Albino rats with special reference to the protective role of *Spirulina platensis*. *Explor. Anim. Med. Res.* 9 (2): 125-136.
- [28] Homeyer, A., Nasr, P., Engel, C., Kechagias, S., Lundberg, P., Ekstedt, M., ... & Lundström, C. (2017). Automated quantification of steatosis: agreement with stereological point counting. *Diagnostic pathology*, 12 (1), 1-10.
- [29] Korany, R.M.S., Ahmed, K.S., El Halawany, H.A. and Ahmed, K.A. (2019). Pathological and immunohistochemical studies on the ameliorating effect of *Spirulina platensis* against arsenic induced reproductive toxicity in female albino rats. *Inter. J. Vet. Sci.*, 8, pp.113-119.
- [30] Madkour, D. A., Ahmed, M. M., Orabi, S. H., Sayed, S. M., Korany, R. M., & Khalifa, H. K. (2021). Nigella sativa oil protects against emamectin benzoate-Induced neurotoxicity in rats. *Environmental Toxicology*, 36(8), 1521-1535.
- [31] Azouz, R. A., & Korany, R. (2021). Toxic impacts of amorphous silica nanoparticles on liver and kidney of male adult rats: an in vivo study. *Biological Trace Element Research*, 199(7), 2653-2662.
- [32] Machado, A. R., Pinheiro, A. C., Vicente, A. A., Souza-Soares, L. A., & Cerqueira, M. A. (2019). Liposomes loaded with phenolic extracts of *Spirulina* LEB-18: Physicochemical characterization and behavior under simulated gastrointestinal conditions. *Food research international*, 120, 656-667.
- [33] Salama, H. H., Elsaid, M. M., Abdel Hamid, S. M., Abozed, S. S., & Mounier, M. (2020). Effect of fortification with sage loaded liposomes on the chemical, physical, microbiological properties and cytotoxicity of yoghurt. *Egyptian Journal of Chemistry*, 63(10), 3879-3890.
- [34] Krämer, S. D., Jakits-Deiser, C., & Wunderli-Allenspach, H. (1997). Free fatty acids cause pH-dependent changes in drug-lipid membrane interactions around physiological pH. *Pharmaceutical research*, 14(6), 827-832.
- [35] Mishra, A., Ram, S., & Ghosh, G. (2009). Dynamic light scattering and optical absorption in biological nanofluids of gold nanoparticles in poly (vinyl pyrrolidone) molecules. *The Journal of Physical Chemistry C*, 113(17), 6976-6982.
- [36] Assis, L. M. D., Machado, A. R., Motta, A. D. S. D., Costa, J. A. V., & Soares, L. A. D. S. (2014). Development and characterization of nanovesicles containing phenolic compounds of microalgae *Spirulina* strain LEB-18 and *Chlorella pyrenoidosa*.
- [37] Ismail, E. A., Aly, A. A., & Atallah, A. A. (2020). Quality and microstructure of freeze-dried yoghurt fortified with additives as protective agents. *Heliyon*, 6(10), e05196.
- [38] Koç, B., Sakin-Yilmazer, M., Kaymak-Ertekin, F., & Balkır, P. (2014). Physical properties of yoghurt powder produced by spray drying. *Journal of food science and technology*, 51(7), 1377-1383.
- [39] Ergun, K., Tiryaki-Gunduz, G., Sakin-Yilmazer, M., DIRIM, S., & Kaymak-Ertekin, F. (2013). Freeze drying of yoghurt with candied chestnut puree: survival of lactic acid bacteria and determination of physical properties. *Italian Journal of Food Science*, 25(4).
- [40] Rybka, S., & Kailasapathy, K. (1995). The survival of culture bacteria in fresh and freeze-dried AB yoghurts. *Australian journal of dairy technology*, 50(2), 51.
- [41] Venir, E., Del Torre, M., Stecchini, M. L., Maltini, E., & Di Nardo, P. (2007). Preparation of freeze-dried yoghurt as a space food. *Journal of food engineering*, 80(2), 402-407.
- [42] Haswell, C., Ali, A., Page, R., Hurst, R., & Rutherford-Markwick, K. (2021). Potential of Beetroot and Blackcurrant Compounds to Improve Metabolic Syndrome Risk Factors. *Metabolites*, 11(6), 338.
- [43] Olumese, F., & Oboh, H. (2016). Effects of daily intake of beetroot juice on blood glucose and hormones in young healthy subjects. *Ann Trop Pathol*, 26, 455-462.
- [44] Kaur, J. (2014). A comprehensive review on metabolic syndrome. *Cardiology research and practice*, 2014.
- [45] Salazar, M. R., Carbajal, H. A., Espeche, W. G., Leiva Siniegui, C. E., March, C. E., Balbín, E., ... & Reaven, G. M. (2013). Comparison of the abilities of the plasma triglyceride/high-density lipoprotein cholesterol ratio and the metabolic syndrome to identify insulin resistance. *Diabetes and Vascular Disease Research*, 10(4), 346-352.
- [46] Timmers, S., De Vogel-van Den Bosch, J., De Wit, N., Schaart, G., Van Beurden, D., Hesselink, M., ... & Schrauwen, P. (2011). Differential effects of saturated versus unsaturated dietary fatty acids on weight gain and myocellular lipid profiles in mice. *Nutrition & diabetes*, 1(7), e11-e11.
- [47] Gunawan, S., Santoso, A., & Wijaya, A. (2011). The Correlation of Gamma-Glutamyl Transferase (γ -GT), Glutathione Peroxidase (GPx) and Total Antioxidant Status (TAS) with Inflammatory Marker in Individuals with Metabolic Syndrome. *The Indonesian Biomedical Journal*, 3(1), 57-63.
- [48] Echeverría, F., Valenzuela, R., Bustamante, A., Álvarez, D., Ortiz, M., Soto-Alarcon, S. A., ... & Videla, L. A. (2018). Attenuation of high-fat diet-induced rat liver oxidative stress and steatosis by combined hydroxytyrosol-(HT-) eicosapentaenoic acid supplementation mainly relies on HT. *Oxidative Medicine and Cellular Longevity*, 2018.
- [49] Clifford, T., Howatson, G., West, D. J., & Stevenson, E. J. (2015). The potential benefits of red beetroot

- supplementation in health and disease. *Nutrients*, 7(4), 2801-2822.
- [50] Amin, A. R., Kassab, R. B., Abdel Moneim, A. E., & Amin, H. K. (2020). Comparison among garlic, berberine, resveratrol, Hibiscus sabdariffa, genus zizyphus, hesperidin, red beetroot, catha edulis, portulaca oleracea, and mulberry leaves in the treatment of hypertension and type 2 DM: a comprehensive review. *Natural Product Communications*, 15(4), 1934578X20921623.
- [51] Velázquez, K. T., Enos, R. T., Bader, J. E., Sougiannis, A. T., Carson, M. S., Chatzistamou, I., & Murphy, E. A. (2019). Prolonged high-fat-diet feeding promotes non-alcoholic fatty liver disease and alters gut microbiota in mice. *World journal of hepatology*, 11(8), 619.
- [52] El-Maksoud, A. A. A., Korany, R. M., El-Ghany, I. H. A., El-Beltagi, H. S., & Ambrósio F. de Gouveia, G. M. (2020). Dietary solutions to dyslipidemia: Milk protein-polysaccharide conjugates as liver biochemical enhancers. *Journal of Food Biochemistry*, 44(3), e13142.
- [53] Elmas, M. A., Cakıcı, S. E., Dur, I. R., Kozluca, I., Arınc, M., Binbuga, B., ... & Ercan, F. (2019). Protective effects of exercise on heart and aorta in high-fat diet-induced obese rats. *Tissue and Cell*, 57, 57-65.
- [54] Santana, A. B. C., Souza Oliveira, T. C. D., Bianconi, B. L., Barauna, V. G., Santos, E. W. C. O., Alves, T. P., ... & Lacchini, S. (2014). Effect of high-fat diet upon inflammatory markers and aortic stiffening in mice. *BioMed research international*, 2014.
- [55] Al-Harbi, L. N., Alshammari, G. M., Al-Dossari, A. M., Subash-Babu, P., Binobead, M. A., Alhussain, M. H. & Shamlan, G. (2021). Beta vulgaris L.(Beetroot) Methanolic Extract Prevents Hepatic Steatosis and Liver Damage in T2DM Rats by Hypoglycemic, Insulin-Sensitizing, Antioxidant Effects, and Upregulation of PPAR α . *Biology*, 10(12), 1306.
- [56] Matarese, G., Moschos, S., & Mantzoros, C. S. (2005). Leptin in immunology. *The Journal of Immunology*, 174(6), 3137-3142.
- [57] Considine, R. V., Sinha, M. K., Heiman, M. L., Kriauciunas, A., Stephens, T. W., Nye, M. R., ... & Caro, J. F. (1996). Serum immunoreactive-leptin concentrations in normal-weight and obese humans. *New England Journal of Medicine*, 334(5), 292-295.
- [58] Pradhan, A. D. (2014). Sex differences in the metabolic syndrome: implications for cardiovascular health in women. *Clinical chemistry*, 60(1), 44-52.
- [59] Strimbu, K., & Tavel, J. A. (2010). What are biomarkers?. *Current Opinion in HIV and AIDS*, 5(6), 463.
- [60] Sadri, H., Goodarzi, M. T., Salemi, Z., & Seifi, M. (2017). Antioxidant effects of biochanin A in streptozotocin induced diabetic rats. *Brazilian Archives of Biology and Technology*, 60.
- [61] Albrahim, T., & Alonazi, M. A. (2020). Role of beetroot (*Beta vulgaris*) juice on chronic nanotoxicity of silver nanoparticle-induced hepatotoxicity in male rats. *International Journal of Nanomedicine*, 15, 3471.
- [62] Owumi, S. E., & Dim, U. J. (2019). Manganese suppresses oxidative stress, inflammation and caspase-3 activation in rats exposed to chlorpyrifos. *Toxicology Reports*, 6, 202-209.
- [63] Baxmann, A. C., Ahmed, M. S., Marques, N. C., Menon, V. B., Pereira, A. B., Kirsztajn, G. M., & Heilberg, I. P. (2008). Influence of muscle mass and physical activity on serum and urinary creatinine and serum cystatin C. *Clinical Journal of the American Society of Nephrology*, 3(2), 348-354.
- [64] Seo, J. A., Song, S. W., Han, K., Lee, K. J., & Kim, H. N. (2014). The associations between serum zinc levels and metabolic syndrome in the Korean population: findings from the 2010 Korean National Health and Nutrition Examination Survey. *PLoS one*, 9(8), e105990.
- [65] Bao, B., Prasad, A. S., Beck, F. W., Fitzgerald, J. T., Snell, D., Bao, G. W., ... & Cardozo, L. J. (2010). Zinc decreases C-reactive protein, lipid peroxidation, and inflammatory cytokines in elderly subjects: a potential implication of zinc as an atheroprotective agent. *The American journal of clinical nutrition*, 91(6), 1634-1641.
- [66] Moley NMG, Kelle H. Maternal obesity, infertility and mitochondrial dysfunction: potential mechanisms emerging from mouse model systems. *Molecular human reproduction*. 2013; 19: 486-94.
- [67] Tamanini C, De AM. Angiogenesis in developing follicle and corpus luteum. *Reproduction in Domestic Animals*. 2004; 39: 206.
- [68] Robinson RS, Woad KJ, Hammond AJ, Laird M, Hunter MG, Mann GE Angiogenesis and vascular function in the ovary. *Reproduction*. 2009; 138: 869-81.
- [69] Qiu Y, Seager M, Osman A, Castlemiller J, Bevan H, Tortonese DJ, Ovarian VEGF(165)b expression regulates follicular development, corpus luteum function and fertility. *Reproduction*. 2012; 143: 501-11.
- [70] Fu Y, Lai Y, Wang Q, Liu X, He W, Zhang H, et al. Overexpression of clusterin promotes angiogenesis via the vascular endothelial growth factor in primary ovarian cancer. 2013; 7: 1726.
- [71] Kalra S, Aggarwal S, Khandelwal D. Thyroid dysfunction and type 2 diabetes mellitus: screening strategies and implications for management. *Diabetes Ther*. 2019;10(6):2035-44. <https://doi.org/10.1007/s13300-019-00700-4>.
- [72] Zhang H, Yi M, Zhang Y, Jin H, Zhang W, Yang J, Yan L, Li R, Zhao Y and Qiao J, 2016. High-fat diets exaggerate endocrine and metabolic phenotypes in a rat model of DHEA-induced PCOS. *Reproduction* (2016) 151 431-441
- [73] Hilal G, Fatma T, Ferruh Y, Sabire G, Yüke A., 2019. Effect of high-fat diet on the various morphological parameters of the ovary. *Anatomy and cell biology*, <https://doi.org/10.5115/acb.19.082>
- [74] Li Q, Guo S, Yang C, Liu X, Chen X, He J, Tong C, Ding Y, Peng C, Geng Y, Mu X, Liu T, Li F, Wang Y,

-
- Gao R, 2021. High-fat diet-induced obesity primes fatty acid β oxidation impairment and consequent ovarian dysfunction during early pregnancy. *Ann Transl Med* 2021; 9 (10):887 | <http://dx.doi.org/10.21037/atm-21-2027>
- [75] Kumar S, Kumari S, Dubey NK, Usha D (2020). Anti-Diabetic and Haematinic Effects of Beetroot Juice (*Beta vulgaris* L.) in Alloxan Induced Type-1 Diabetic Albino Rats. *J. Diabetes Res. Ther.* 2020, 6, 1–3.